Aerodynamic Characteristics of a Delta Wing with Arc Camber for Mars Exploration

Takao Unoguchi,*[1] Shogo Aoyama,*[1] Hiroshi Suemura,*[1] Gouji Yamada,*[1] Takashi Matsuno*[1]
Shigeru Obayashi*[2] and Hiromitsu Kawazoe*[1]

*[1] Tottori University, 4-101 Koyama-Minami, Tottori, 680-8552, Japan
*[2] Tohoku University, Katahira 2-1-1, Sendai, 980-8577, Japan
Email address:M11T1005B@edu.tottori-u.ac.jp

Abstract

In this research, we propose a delta wing with an arc camber to explore the Mars in flight at low Reynolds number of 1.0×10^4 order. The research focuses on L/D of a cambered delta wing to get a wide cross range for the Mars exploration by computational analysis and aerodynamic force measurements using a newly developed three-component force balance. The CFD results show that L/D of the delta wing with an arc camber is much better than the no-camber delta wing at a low angle of attack. Especially, the wing with the camber rate of 5% gives the best performance. The validation results by the EFD approach supports the CFD analysis.

Key words: Delta wing, Arc camber, Aerodynamics, Mars exploration, Three-component force balance

1. Introduction

Mars exploration by an airplane is expected as one of prospective methods, because it will enable to explore wide area of the Mars compared with a method by a land rover vehicle [1-3]. Such the airplane needs a wing suitable for the flight at a low Reynolds number in the Mars atmosphere. On the other hand, considering a high speed flight at a high altitude and performance of a wide cross range, a delta wing with a high ratio of lift to drag should be one of the candidates. Furthermore, a light, simple, and structurally strong wing is favorable for the carry to the Mars and the certain operation.

Supposing a Mars airplane which flies from high to low altitude in various speed, we have proposed a delta wing with a variable swept back angle of the leading edge. Furthermore, focusing on a low altitude flight at low speed in the Mars, a delta wing, the camber of which is changeable, has been also suggested to get a suitable performance of the ratio of lift to drag to the flight just above the Mars surface. In this paper, a delta wing with thin thickness and an arc-shape chord was investigated by the numerical and the experimental studies in the condition of a low Reynolds number [4-5]. Analysis by the computational fluid dynamics was carried out to study the characteristics of a thin delta wing with arc camber in such a low Reynolds number as the order of 1.0×10^4. Especially, we want to know what rate of the camber gives the maximum L/D. On the other hand, the experimental study was undertaken to make sure the prediction of the numerical analysis.

2. Prediction by the CFD Approach

2.1 Numerical Procedure

The plane shape of the thin delta wing of the research is shown in Fig.1, which has the swept-back angle of 60 degrees and the root chord length of 260 mm. The delta wing shown in Fig.1(a) has an arc-shape chord. The ratio of the maximum camber of the delta wing to the root chord, which is called as a camber ratio in the research, was changed from 0 to 15%. The aerodynamic performances of such the arc-shape cambered delta wings with a camber ratio were expected by numerical simulations based on the computational fluid dynamics (CFD). The higher the lift-drag ratio (L/D) becomes, the wider the cross range is. The delta wing in Fig.1(b) is a flat-plate type which was also investigated in the both of the numerical and the experimental approaches as a base delta wing. The CFD condition and the camber ratio for the CFD analysis are indicated in Tables 1 and 2.

The airflow around a delta wing were simulated for the various cases listed in Table 2 by the STAR-CCM+ code which is capable of generating grids and post processing the results. Figure 2 shows the computational grids for the case of the camber ratio of 5%. Incompressible Navier-Stokes equation without a turbulence model was used for these simulations.

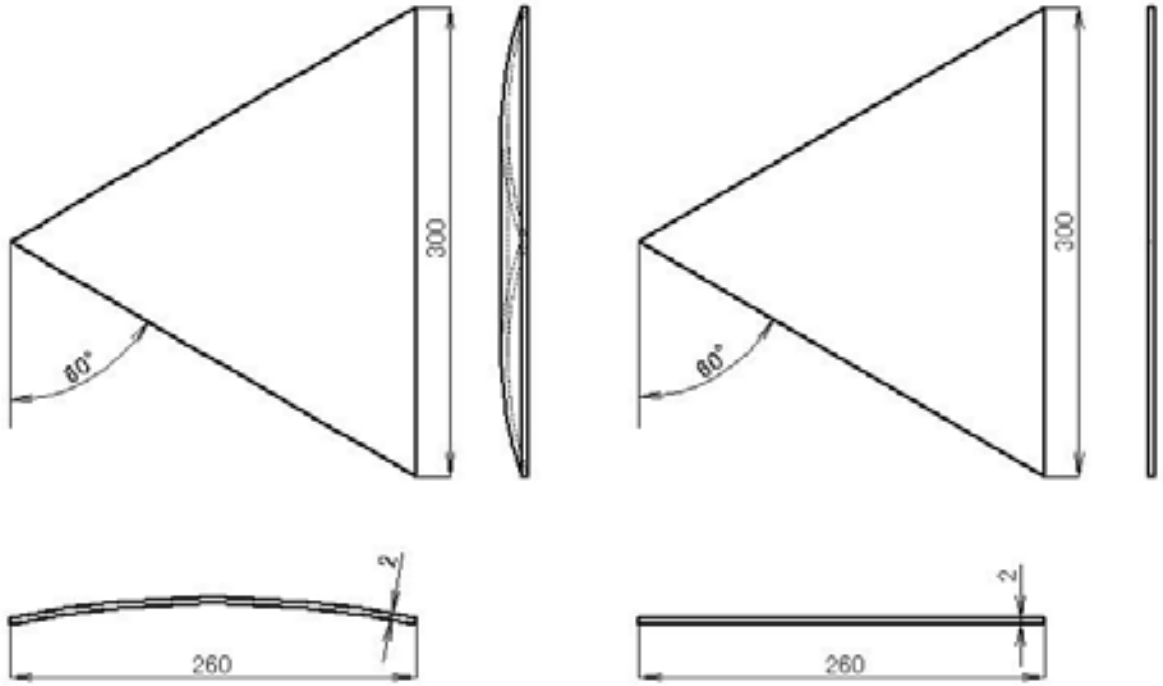

(a) Cambered delta wing **(b) Flat delta wing**

Fig.1 Delta wing geometry

Table 1 CFD condition for Mars atmosphere

Atmospheric condition	component	CO_2 100%
	density	0.0155 [kg/m^3]
	velocity	34 [m/s]
	pressure	700 [Pa]
	viscosity	1.36×10-5 [Pa・S]
	Reynolds number	1.0×10^4
Number of numerical cells		500,000 for the half span (Fig.2)

Table 2 Camber ratio in CFD approach

camber ratio	camber [mm]	root chord [mm]	Re
0%	0	260	1.0×10^4
0.5%	1.3	260	1.0×10^4
1%	2.6	260	1.0×10^4
3%	7.8	260	1.0×10^4
5%	13	260	1.0×10^4
7%	18.2	260	1.0×10^4
10%	26	260	1.0×10^4
15%	39	260	1.0×10^4

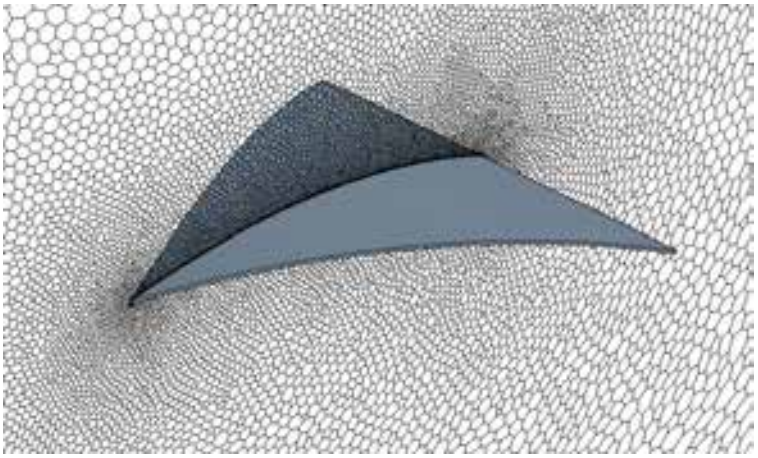

Fig.2 Volume mesh condition around the delta wing (camber ratio of 5%)

2.2 CFD Results

Figure 3 shows the L/D versus a camber ratio of the delta wings in the case of the Reynolds number of 1.0×10^4. The delta wing with an arc camber obtained higher performance than the flat delta wing at a low angle of attack. Especially, the delta wing with the camber ratio of nearby 5% gives the best performance compared to the other cambered wings at the all of the attack angle, namely 0, 5, and 10 degrees.

Figure 4 shows the longitudinal three components of aerodynamic force and moment (C_L, C_D, C_M) and L/D versus an angle of attack for the representative camber ratios of 0, 3, 5, and 7 %. It was found from the results that the delta wing with a large camber obtained high lift because of its effect similar to a flap. However, drag increases more rapidly than lift at an attack angle over 5 degrees. Therefore, the L/D of a large cambered delta wing decreases at a high angle of attack as shown in Fig.4(d). These results show that an optimum camber ratio exists to obtain a maximum L/D and it becomes about 5% in this study. Moreover, the change of L/D is very small at the attack angle between 0 and 5 degrees.

The results mentioned above are based on only the CFD analysis and it is, therefore, necessary to validate them by the experimental fluid dynamics (EFD) approach. However, experimental measurements of aerodynamic force and moment using a force balance should be very difficult for small lift and drag due to a low Reynolds number [6-9]. For the difficulties we newly designed and made a compact force balance to measure them. In the next chapter the force balance will be mentioned shortly and the validation to the CFD results by the EFD approach with the force balance will be described.

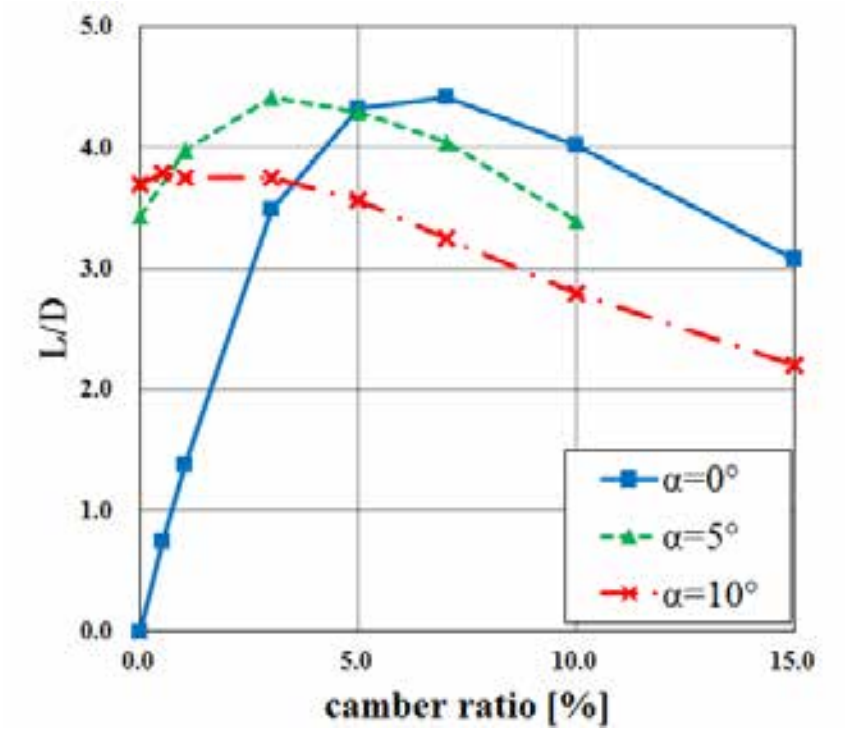

Fig.3 L/D characteristics with a camber ratio

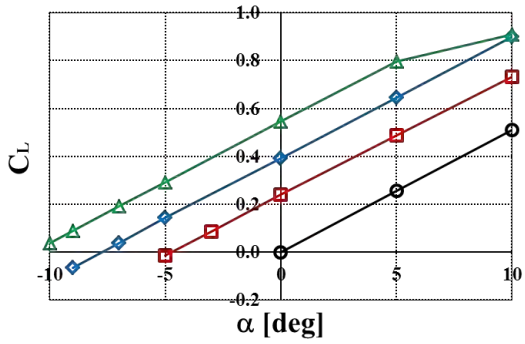

(a) Lift

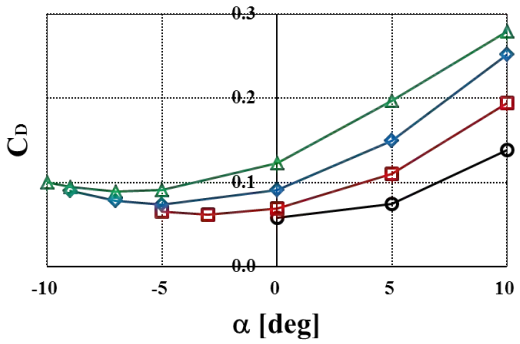

(b) Drag

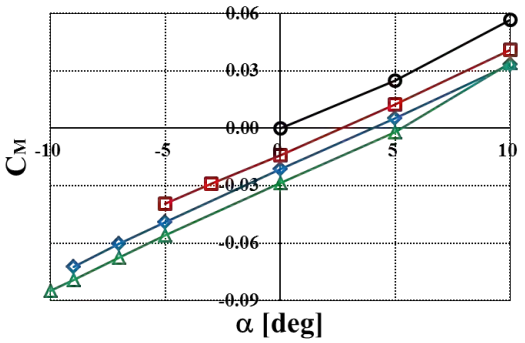

(c) Pitching moment

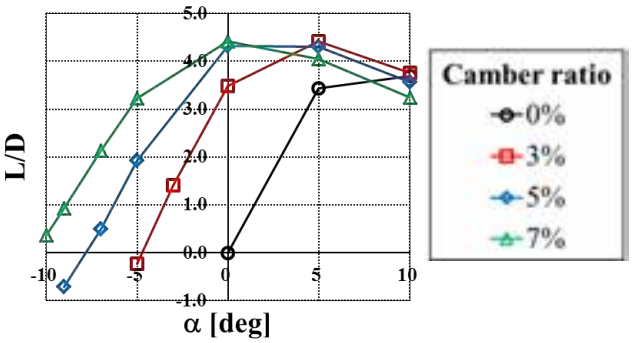

(d) L/D

Fig.4 Aerodynamic characteristics of the cambered delta wings ($\mathrm{Re}=1.0\times10^{4}$)

3. Validation by the EFD Approach

3.1 Compact Force Balance

In the case of the low Reynolds number of 1.0×10^4 with the size of the delta wing shown in Fig.1, lift, drag and pitching moment were estimated no more than 0.15 N, 0.04 N, and 1.6×10^{-3} Nm respectively. A new type of force balance was then designed for the measurement as shown in Fig.5 and was made as shown in Fig.6. The ring part of the force balance has the diameter of 21 mm with the thickness of 0.5 mm and the width of 10 mm. Strains at the locations of the symbols F(y) and F(z) in Fig.5 corresponds to drag and lift in the research.

Measurements of aerodynamic force and moment were carried out at the low-speed wind tunnel of Tottori University as shown in Fig.7. The wind tunnel has the test section of 0.6 m $\times$0.6 m. Two delta wing models with an arc camber and no camber were made for the EFD validation measurements, the camber ratio of which is 5%. The no camber model was made of a flat plate with the thickness of 2 mm. These models made of aluminum. The geometrical data of these delta wings are the half size of the CFD research, that is the root chord of 130 mm. Table 3 shows the experimental conditions. Because lift and drag in the condition of the low Reynolds number, 1.0×10^4, became so small to detect by the newly developed force balance, the speed of the wind flow was increased from 1.2 m/s of for the Reynolds number of 1.0×10^4 to 6 m/s and 10 m/s corresponding to the Reynolds number of $5.0\times10^4$and 8.2×10^4 respectively. These are the case name, EXP01 and EXP02, in Table 3, and analysis by the CFD simulation was also carried out for the case of the Reynolds number of 5.0×10^4 in the case of the root chord of 130 mm as shown in Table 3.

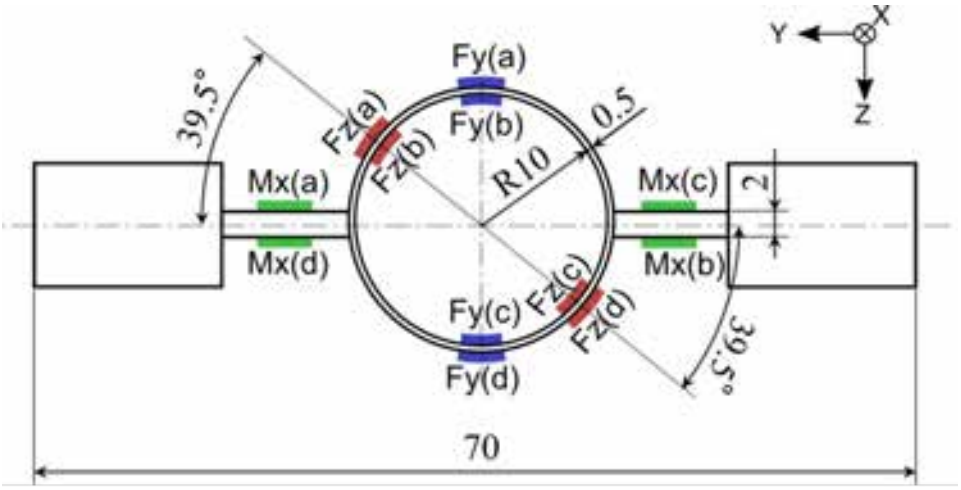

unit: mm

Fig.5 Schematic diagram of the three-component force balance

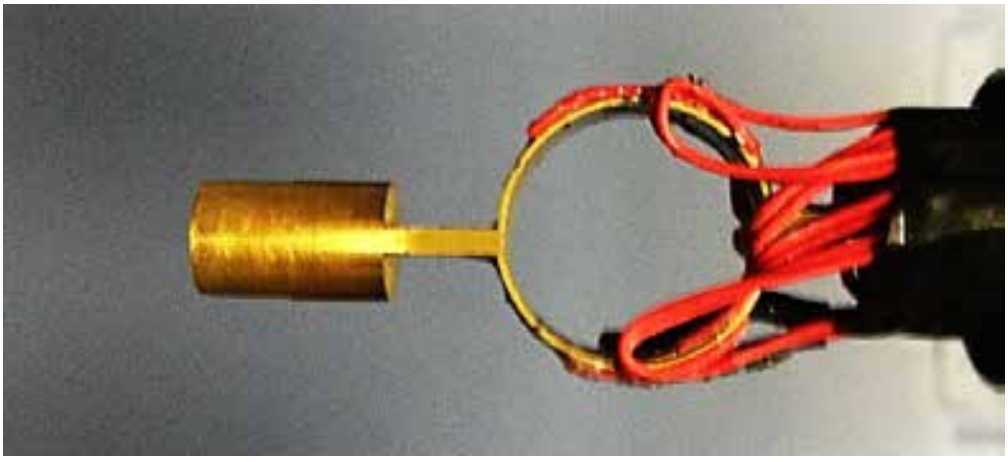

Fig.6 Developed three-component force balance

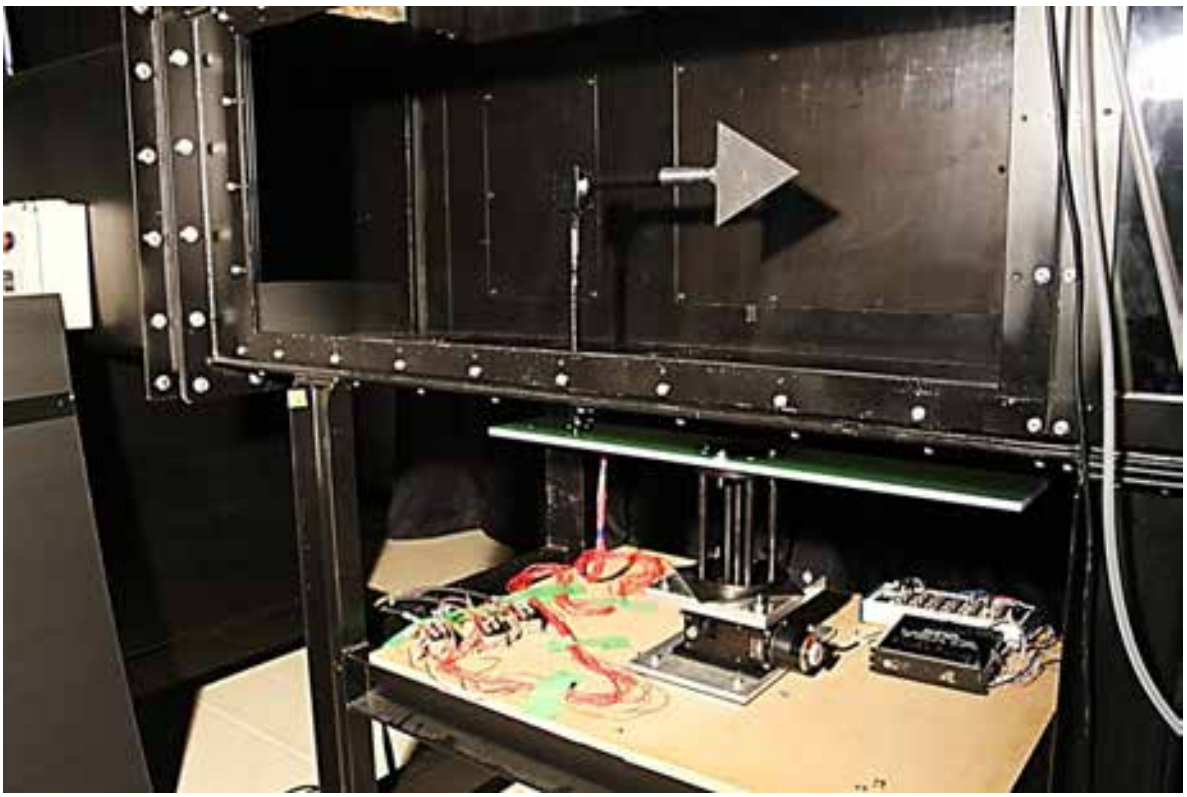

Fig.7 Experimental setup in the test section of the wind tunnel

Table 3 Experimental conditions

case	model	camber [mm]	root chord [mm]	flow velocity [m/s]	Re
EXP01	flat	0	130	10	8.2×10^4
	5% cambered	6.5		10	
EXP02	flat	0	130	6	5.0×10^4
	5% cambered	6.5		6	
CFD	flat	0	130	6	5.0×10^4
	5% cambered	6.5		6	

3.2 EFD Results

Aerodynamic characteristics of the arc camber and the flat delta wings are shown in Fig.8 comparing with the CFD results indicated by the solid and the dotted lines. First, from the results of the lift characteristics of Fig.8(a), it was found that the cambered delta wing gives higher lift than the flat delta wing because of its flap effect as same as the CFD results. The quantitative difference between them, namely about 4%, are almost the same in the EFD and the CFD results similar to those of Fig.4(a). Furthermore, considering the results of the EXP01 and EXP02 which is for the cases of the Reynolds number of 8.2×10^4 and 5.0×10^4, the CFD results of Fig.4(a) for the Reynolds number of 1.0×10^4 can be considered to be quantitatively reasonable values. However, the slopes of the C_L-α by the CFD approach become a little bit gentle compared with the EFD ones. The reason might be due to the assumption of laminar flow in the CFD approach even for vortical flows coming from the leading edge of the delta wing.

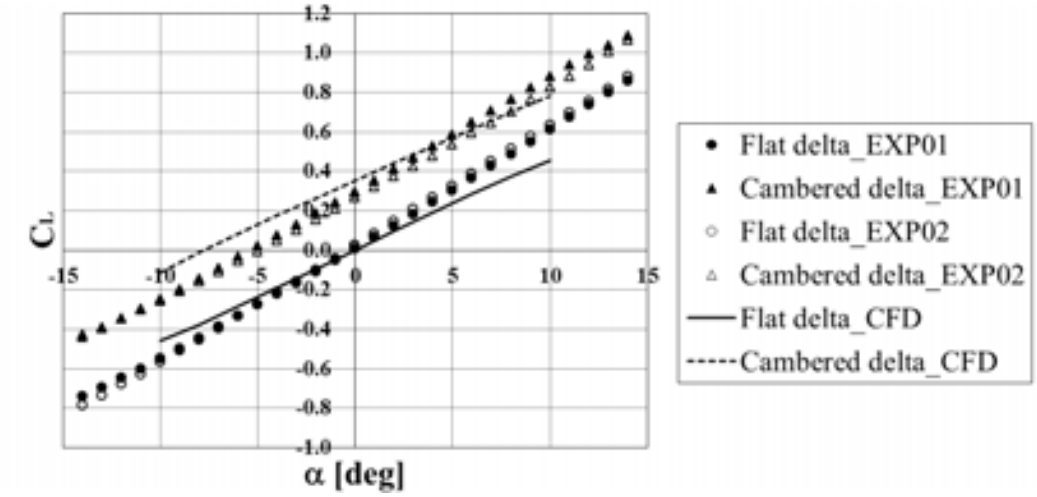

(a) C_L-α curve

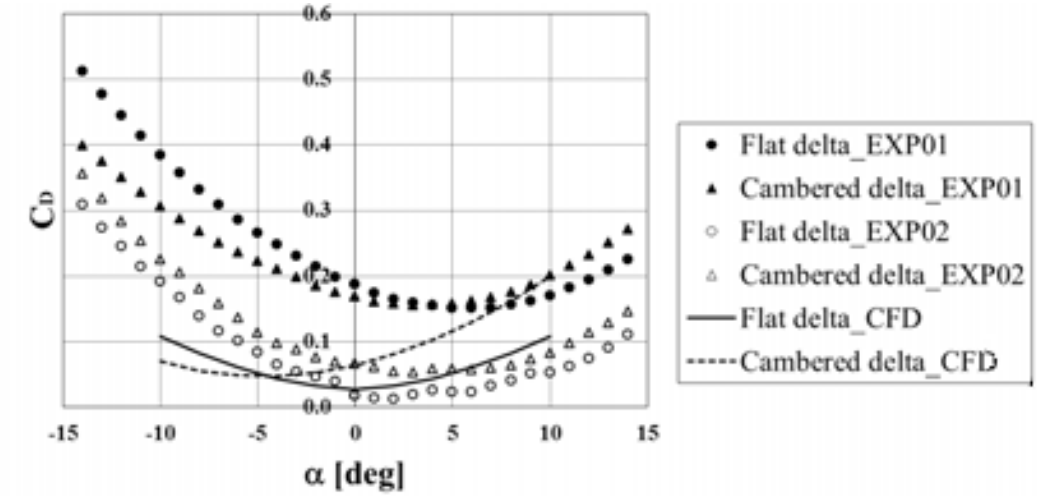

(b) C_D-α curve

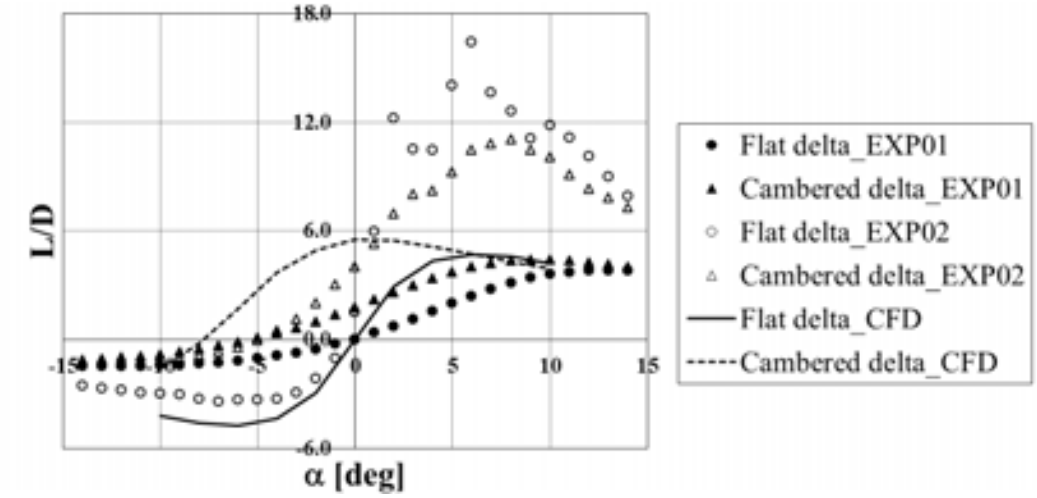

(c) L/D-α curve

Fig.8 Aerodynamic characteristics of the arc camber and the flat delta wings compared with the CFD results

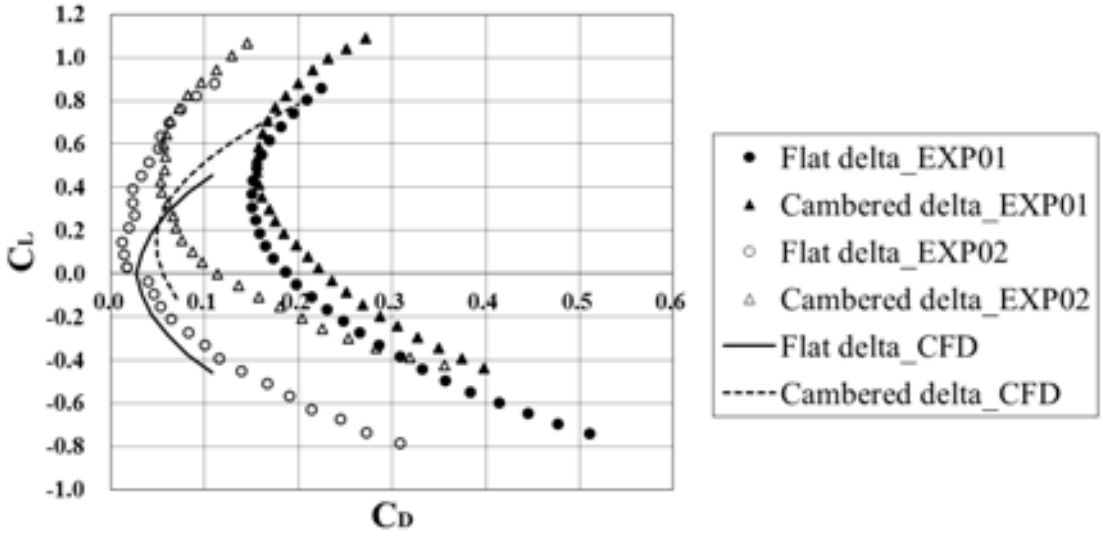

Fig.9 Drag polar curves

Second, the angle of attack to give a minimum C_D for the arc camber delta wing was smaller than the flat delta wing, which should be a cambered effect as shown in Fig.7(b). For example, the minimum C_D of the flat delta in the EXP01 condition is at the attack angle of 6 degrees. On the other hand, the minimum C_D of the arc camber delta wing appears at the attack angle of 3 degrees. These effect also appears in the CFD results in Fig.8(b) as well as in Figs.4(b) and 8(b) for the EXP01. From these results, the CFD analysis can reproduce an actual phenomena quantitatively but involves such an quantitative difference that an attack angle giving a minimum C_D shifts to the smaller side than the both conditions of EXP01 and EXP02.

Third, the L/D of the arc camber delta wing is larger than the flat delta wing except an attack angle over one degree of the EXP02 as shown in Fig.8(c). These effects also appear in the CFD results of Figs.4(d) and 8(c) for the condition of EXP01. The reason for the different result of the EXP02 should be due to the fairly low drag of the flat delta wing at the attack angle over 0 degree in Fig.8(b). It is different from the EXP01 case. It will be one of the future subjects.

With the regard to the difference between the CFD and the EFD results, followings are the summary. The slope of C_L-α is gradual in the CFD approach. The attack angle giving a minimum C_D for the CFD case is smaller than the EFD result and the C_D of the EXP02 becomes larger for the all angles of attack as shown in Fig.8(b). The L/D of the flat delta wing in the EXP02 is much larger than the arc camber delta wing in Fig.8(c). We could consider the reason as follows. It might come from the interference between the wing and the sting with the force balance in the EFD approach. Furthermore, the CFD approach might not simulate correctly the vortical airflows of the delta wing, especially an leading edge separation vortex and such the behavior as vortex breakdown, because the CFD adopts the Navier-Stokes equation without turbulent flow.

Finally, Figure 9 shows the drag polar curves given by C_L and C_D in Fig.8. It suggests that an arc camber delta wing is definitely proper for the flight which needs such the relatively high lift as $C_L \geq 0.5$.

4. Conclusion

A delta wing with an arc camber has been proposed for such a low Reynolds number flight as a flight above the Mars surface and the characteristics were investigated by both the CFD and the EFD approaches. The optimum camber ratio for the flight in the Reynolds number of 1.0×10^4 was studied by the CFD and the resultant validation was inspected by the EFD. As the results, the followings were made sure.

(1) An optimum camber ratio exists according to a flight condition.
(2) The camber ratio of 5% is the best for the delta wing in the research.
(3) The camber acts as a flap and gives a high performance in the flight which needs the high lift such as C_L over 0.5.
(4) The CFD results represent the flow field around the arc camber delta wing qualitatively and some results, although, do not coincide to the EFD results quantitatively.
(5) The reason for the difference might be from the CFD procedure, for example without considering a turbulent flow.

References

[1] Akira Oyama and Kozo Fujii, A Study of Airfoil Design for Future Mars Airplane, AIAA Paper, No.2006-1484, 2006.

[2] Taku Nonomura, Ryoji Kojima, Hiroaki Fukumoto, Akira Oyama and Kozo Fujii, Comparative Study of Aerodynamic Characteristics of Rectangular and Delta Wings under a Low Reynolds Number Condition, Proceedings of 42nd Fluid Dynamics Conference/Aerospace Numerical Simulation Symposium 2010, pp.161-166, 2010. (in Japanese)

[3] Taku Nonomura, Ryoji Kojima, Masayuki Anyoji, Akira Oyama and Kozo Fujii, Aerodynamic Characteristics of Ishii Airfoil (Re=23,000) using LES, J. JSASS-2011-2033, 2011. (in Japanese)

[4] Alain Pelletier and Thomas J. Mueller, Low Reynolds Number Aerodynamics of Low-Aspect-Ratio, Thin/Flat/Cambered-Plate Wings, Jounal of AIRCRAFT, Vol.37, No.5, pp.825-832, September-October 2000.

[5] Makoto Mizoguchi and Yutaka Yamaguchi, Aerodynamic Characteristics of Rectangular Flat Plate Wings in Low Reynolds Number Flows, J. JSASS, Vol.60, No.3, pp.121-127,2012. (in Japanese)

[6] Tomohisa Ohtake, Yusuke Nakae and Tatsuo Motohashi, Nonlinearity of the Aerodynamic Characterristics of NACA0012 Aerofoil at Low Reynolds Numbers, J. JSASS, Vol.55, No.644, pp.439-445, 2007. (in Japanese)

[7] Asei Tezuka, Yasuto Sunada and Kenichi Rinoie, Aerodynamic Characteristics of 4% Cambered-Plate and NACA0012 Airfoil at the Reynolds Numbers Region for Micro Air Vehicles, J. JSASS, Vol.57, No.665, pp.258-265, 2009. (in Japanese)

[8] Tomohisa Ohtake, Yusuke Nakae, Akinori Muramatsu and Tatsuo Motohashi, Flow Field Phenomena Contains Laminar Separation and Separation Bubble on NACA0012 Airfoil at Low Reynolds Number, Proceedings of 42nd Fluid Dynamics Conference/Aerospace Numerical Simulation Symposium 2010, pp.283-286, 2010. (in Japanese)

[9] Yusuke Nakae, Tomohisa Ohtake, Akinori Muramatsu and Tatsuo Motohashi, Three Dimensionalization of the Flow Field around a NACA0012 Airfoil at Low Reynolds Number, J. JSASS, Vol.59, No.692, pp.244-251, 2011. (in Japanese)